Synthesis and Characterization of Waterglass-Based Silica Aerogel Under Heat Treatment for Adsorption of Nitrate from Water: Batch and Column Studies

E. Tohfegar [1], J.S. Moghaddas [1*], E. Sharifzadeh [2], S. Esmaeilzadeh–Dilmaghani [3,4]

[1] *Chemical Engineering Faculty, Sahand University of Technology, P. O. Box: 51335-1996, Sahand, Tabriz, Iran*
[2] *Polymer Research Center, Faculty of Petroleum and Chemical Engineering, Razi University, Kermanshah, Iran*
[3] *Chemical Engineering Faculty, Amirkabir University of Technology, Tehran, Iran*
[4] *Chemical Engineering Department, Koch (Koç) University, Istanbul, Turkey*

ARTICLE INFO	ABSTRACT
	In this work, hydrophobic silica aerogels were synthesized using sol-gel method and drying at ambient pressure. The surface morphology, pore size, and the presence of functional groups on the surface of the nanoparticles were analyzed using FE-SEM, TGA, FT-IR, and EDX, respectively. After calcination at 500 °C, the hydrophilic property of the adsorbents was evaluated by water contact angle measurements. The calcinated silica aerogels were used for adsorption of nitrate from aqueous solution in both batch and continuous processes. In the batch process, the effect of initial nitrate concentration, contact time, pH level, and adsorbent dosage were investigated. Results showed that the nitrate removal percentage increased with the decrement of the pH level and the initial nitrate concentration. On the other hand, increasing the contact time and the adsorbent dosage resulted in higher removal percentage. Accordingly, process optimization resulted in a nitrate removal of 92.2 %. Furthermore, it was found that the equilibrium results were in agreement with the Langmuir isotherm model better than with the Freundlich model and also the adsorption kinetics followed the pseudo-second-order model. In the continuous process, the effects of the input flow rate, the bed height, and the initial nitrate concentration were investigated.

1. Introduction

There are many different components of nitrogen (e.g., ammonia and nitrate) which can be found in water. Fresh sewage contains nitrogen which can turn into ammonia nitrogen through time and then transform to nitrate in aerobic condition [1]. As a naturally created ion, nitrate is highly soluble in water [1, 2]. Nitrate pollutant can be introduced into the surface and underground water resources by agricultural activities, overuse of chemical fertilizers, and inappropriate disposal of

industrial and domestic sewage and animal wastes [3]. According to the World Health Organization (WHO) standards, the amount of nitrate in drinking water should not exceed 45 mg/L because the high level of nitrate can cause many significant disorders in the human body (e.g., blue baby syndrome and digestion cancer) [4]. Some specific characterizations of nitrate ion such as stability and low deposition potential make it quite difficult to be removed by common treating methods (e.g., filtration and lime softening) [5]. Therefore, it is necessary to use some other complicated methods (e.g., ion exchange, reverse osmosis, and electrodialysis) in order to increase the performance of the removing process [6]. However, the mentioned methods suffer from some disadvantages that directly affect their capability to remove nitrate from water resources [7]. Accordingly, applying a wide variety of different adsorbents has been introduced as the primary method for nitrate removal on an industrial scale due to its convenience in the process and cost efficiency [8].

There are several different kinds of adsorbents such as zeolites (with removal percentage of 40 %) [9], activated carbons (29.5 %) [10], and adsorbent clays (22.28 %) [11]. Different types of adsorbent clays are usually used for removing hydrophobic organic pollutants [12]. Most of these adsorbents can reach the maximum value of 40 % of nitrate removal, while this value is 50 % for modified zeolites [13, 14]. Hydro-lactic and chitosan compounds are highly applicable to nitrate removal processes (70-88 %) [15-17]. However, the preheating stage required for maximizing the efficiency of nitrate removal process by chitosan and hydro-lactic adsorbents is quite cost intensive [16, 17]. As another drawback, chitosan

compounds are more efficient in acidic environments which make them essential to neutralizing the acidic outputs before application [17]. Silica Aerogels (SAs) are biocompatible materials that provide a high surface area due to their porous structure and therefore, they can be used for absorbing oil and toxic compounds. On the other hand, requiring no preheating stage or pH level control (best nitrate removal efficiency (89.88 %) at pH=6.8) in nitrate removal processes makes them completely cost-effective and suitable compared to other adsorbents.

Accordingly, in this research, synthesized silica aerogels have been used in order to remove nitrate from water. At first, the nanoparticles were synthesized using sol-gel method and then exposed to the primary surface modification process using Trimethylchlorosilane (TMCS) as a silylating agent. Finally, for extracting the remaining solvents from the gel structure, the drying process was performed under atmospheric pressure [18]. After calcination at 500 $^{\circ}$C, the prepared adsorbents were used to investigate the effect of parameters such as contact time, adsorbent dosage, initial nitrate concentration, pH level, input flow rate, and column length in both batch and continuous nitrate removal processes. Furthermore, the results of Langmuir and Freundlich adsorption isotherm models were compared with equilibrium experimental data and also the pseudo-first-order and the pseudo-second-order kinetic models were used to study the kinetics of the process.

2. Experimental
2.1. Materials
Sodium silicate (Na$_2$SiO$_3$, ρ =1.35 g/cm^3, pH =11-11.5), Trimethychlorosilane (TMCS,

$\rho = 0.86$ g/cm^3) as silylating agent, n-hexane ($\rho = 0.66$ g/cm^3, > 96 %), Isopropyl alcohol ($\rho = 0.786$ g/cm^3, > 99.8 %), and Tartaric acid ($\rho = 1.76$ g/cm^3, pH = 1.6, >99.5) were purchased from Merck. Moreover, Sodium nitrate (Sigma Aldrich, > 99 %) was used as received.

2.2. Aerogel synthesis method

Generally, the synthesis of silica aerogel consists of three steps: (I) gel preparation, (II) ageing, and (III) drying. At first, sodium silicate was mixed with deionized water (volume ratio of 1:4) to prepare sodium silicate solution. Then, the tartaric acid solution was prepared via mixing tartaric acid with an equal mole of deionized water. The sodium silicate solution was poured in a beaker under stirring and the tartaric acid solution was added to it dropwise till the colour of the solution was changed to milky white. The obtained solution was transferred to a closed Teflon container and then, the ageing process was done at 55 °C for 3 hours in order to form a strong silica gel structure. The provided gel was washed with deionized water every 6 hours during 24 hours in order to extract the residual sodium tartrate. Then, the silica gel was placed in a mixture of isopropyl alcohol and normal hexane (volume ratio of 1:1) at 50 °C for 24 hours to keep up its strength and preventing it from shrinkage. The chemical modification of the gel was then performed in a mixture of n-hexane and TMCS (volume ratio of 1:4) at 55 °C for 24 hours. Finally, the system temperature was increased from 50 °C to 120 °C for 2 hours till the gel dried [18, 19]. The prepared silica aerogels were calcinated at 500 ^{o}C for 3 hours to replace the existing superficial methyl groups with hydroxyl groups [20].

2.3. Characterization methods

The surface morphology of the synthesized silica aerogels was investigated using field emission scanning electron microscopy (MIRA3 FE-SEM, Tuscan, Czech) before and after the calcination process. Fourier Transform Infrared Spectroscopy (FT-IR) analysis was used to characterize the chemical nature of the products. Thermogravimetric Analysis (TGA) was carried out from ambient temperature up to 800 °C (heating rate of 10 °C/min) using a Pyres 1 thermogravimetric analyzer (PerkinElmer, USA). EDX tests were conducted using the FE-SEM device. Contact angle measurements were also conducted in order to determine the hydrophilic and hydrophobic characteristics of aerogel samples (PGX, Thwing-Albert-instrument Co, SWEDE).

Furthermore, the nitrate concentration in water was measured using a UV spectrophotometer device (Lambda 365, PerkinElmer). This method implies that the absorbance of the nitrate solution samples to be measured at 200 nm (strong absorbance of the nitrate ion) and 270 nm (where organic matters absorb strongly and the absorption of nitrate can be neglected). By subtracting the two obtained values, it is possible to estimate absorption due to nitrate [21].

2.4. Nitrate adsorption in the batch process

In order to investigate the batch process, the most effective parameters for the nitrate removal efficiency such as initial nitrate concentration, the pH level of the prepared nitrate solution samples, adsorbent dosage, and contact time were selected [4, 22, 23]. After performing the experiments and evaluating the effects of the selected parameters on the process, the adsorbents were separated by centrifuging at 1800 rpm

and a microsyringe filter of 0.2 micrometer. The nitrate removal percentage was obtained using Equation (1) [24]:

$$R\% = \left(\frac{C_0 - C}{C_0} \right) \times 100 \qquad (1)$$

where C_0 and C denote initial and time dependent nitrate concentrations.

2.5. Adsorption kinetics in the batch process

Equilibrium kinetics has a significantly important role in the adsorption process and can be used to determine the equilibrium time and the controlling mechanism [16]. The investigation of adsorption kinetics was conducted using 1 L of nitrate solution (100 mg.L^{-1}) comprising 3 g of the prepared hydrophilic silica aerogel as the adsorbent. The suspension was stirred using a mixer at ambient temperature and meanwhile, in different specific time periods, several samplings were performed. The sampling process was continued till the equilibrium was reached (the final nitrate concentration in the *i+1* sample = the final nitrate concentration in the *i* sample). The adsorbents were then removed using centrifuging and the nitrate concentration was measured via UV spectrophotometer.

2.6. Adsorption isotherm in the batch process

The equilibrium isotherms were investigated using Langmuir and Freundlich isotherm models. To this end, 3 g of the adsorbent was added to solution samples (1 L) comprising different amounts of nitrate (100-500 mg.L^{-1}) and then stirred at ambient temperature. After reaching the equilibrium, the adsorbents were separated by centrifuging.

2.7. Nitrate adsorption in the continuous process

The continuous nitrate adsorption processes were carried out using a 600 mm long Pyrex column with a diameter of 14 mm (as the adsorption column). The required amount of the adsorbent was weighted and then added to the column. A filter was installed at the bottom end of the column to prevent the water flow to take out the adsorbents and also to stabilize them. Furthermore, a flow meter was used to control the input flow rate of the solution comprising specific amounts of nitrate. In order to reach a stable bed height, a deionized water flow was introduced into the column (for 10 min) before starting the main experiments. Figure 1 represents a schematic of the applied setup in the continuous process.

At the beginning of the process, the maximum rate of the mass transfer occurs at the entrance of the bed. However, as time passes, the entrance zone becomes saturated and therefore, the adsorption will occur in further zones. The zone responsible for the highest amounts of the concentration variation (from $C/C_0=0.95$ to $C/C_0=0.05$) is called the mass transfer area. The required time spans to reach $C/C_0=0.05$ and $C/C_0=0.95$ are named breakthrough and saturation times of the bed, respectively [25, 26]. The adsorbent capacity up to the exhaustion point (q_{sat}) can be determined using Equation (2) [27]:

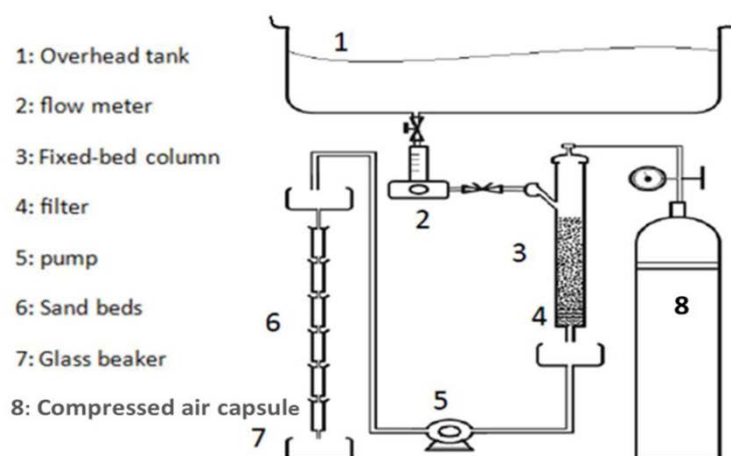$$q_{sat} = Q \left(C_0 t_{sat} - \int_0^{t_{sat}} C dt \right) / m \qquad (2)$$

where Q is the flow rate and m denotes the amount of adsorbent.
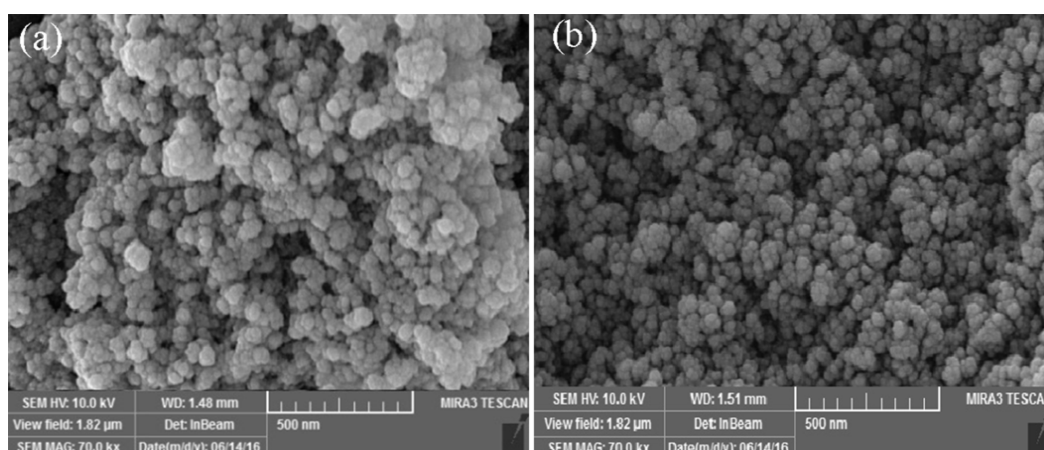
3. Results and discussion

The shape and size of the synthesized hydrophobic silica aerogels were investigated using FE-SEM images, which showed that the

nanoparticles were spherical with a size of 10-20 nm (Figure 2a). Furthermore, by evaluating the nanoparticles after the calcination process, it was revealed that the process reduced the nanoparticle size (Figure 2b) [28].

1: Overhead tank
2: flow meter
3: Fixed-bed column
4: filter
5: pump
6: Sand beds
7: Glass beaker
8: Compressed air capsule

Figure 1. The designed setup for continuous nitrate removal process.

Figure 2. FE-SEM images of the synthesized silica aerogels (a) before and (b) after calcination process.

The FT-IR results of both hydrophilic and hydrophobic silica aerogel samples are represented in Figure 3. As it is clear, the peaks at wavenumbers of 1086 cm^{-1}, 847 cm^{-1}, and 460 cm^{-1} can be assigned to Si–O–Si asymmetric stretching, symmetric stretching, and bending vibrations, respectively [29-31], showing sillies network in the silica aerogel structure. The absorption peak at 1260 corresponds to the Si–C bond and the peaks at 2980 and 1450 cm^{-1} represent C–H bond [32]. Accordingly, it is clear that the surface modification stage using TMCS was successfully accomplished and the surface of the synthesized nanoparticles was completely hydrophobic. After the calcination process, the broad absorption peak at around 3500 and 1600 cm^{-1} denotes the presence of O–H groups on the surface of the nanoparticles which also justify their hydrophilicity [32]. Moreover, the absence of the characterizing peaks of C-H and Si-C bonds in the FT-IR results of calcinated samples proves the oxidation of methyl groups due to heating treatments [28].

In order to further investigate the

characteristics of the synthesized silica aerogels, a contact angle test was also performed. To this end, it was essential to prepare some coated surfaces with both hydrophobic and hydrophilic nanoparticles.

The coating process was conducted using a coating device on the glass slides based on our previously proposed method (Figure 4) [33].
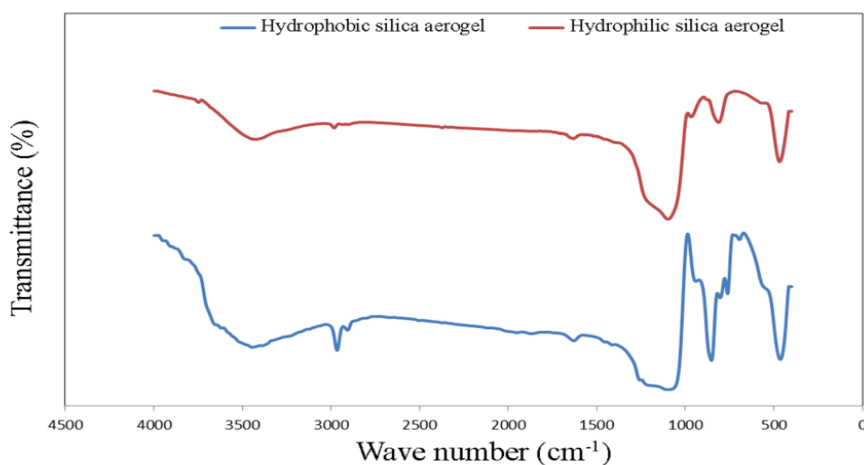
Figure 3. FT-IR spectra of the hydrophobic and hydrophilic silica aerogels.
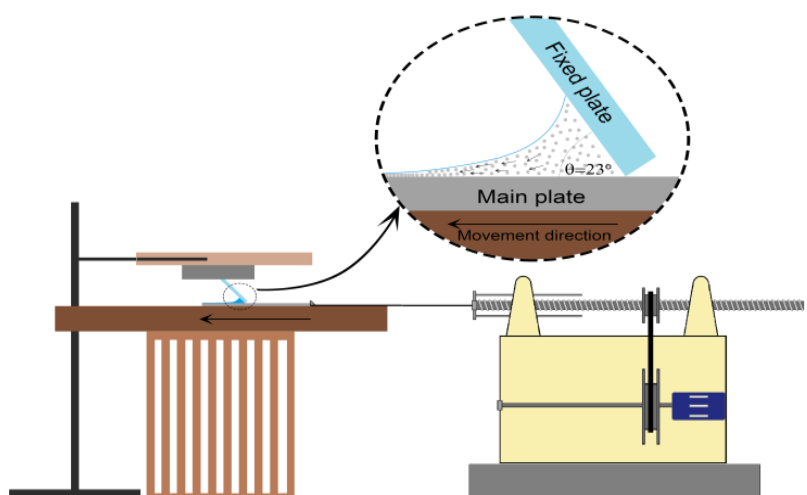
Figure 4. Schematic of the device applied to coating the surface of the glass slides with nanoparticles [40].

As shown in Figure 5a, the water droplet formed a contact angle of 154° on the coated surface with hydrophobic nanoparticles, while this value was less than 13° on the coated surface with hydrophilic nanoparticles (Figure 5b).

Figure 6 represents the results of the TGA test for both hydrophilic and hydrophobic silica aerogel samples. The primary weight loss of both samples was attributed to both the evaporation of residual solvents in the

nanoparticle pores and the surface humidity [34]. Furthermore, the oxidation of methyl groups resulted in significant weight loss in the hydrophobic sample (starts at 390 ^{o}C) while there is no similar weight loss for the hydrophilic sample. This shows that the temperature and the time duration of the calcination process were perfectly set.

Figure 7 represents the results of EDX test which was used for distinguishing the elements on the surface of the hydrophilic and

hydrophobic samples. As it can be seen in Figure 7a, the presence of Si, O, and C peaks indicates the existence of methyl groups on the surface of silica aerogel. On the other hand, there is no carbon characterizing peak in the EDX result of the hydrophilic sample (Figure 7b), while the O peak is amplified due to the presence of OH groups.
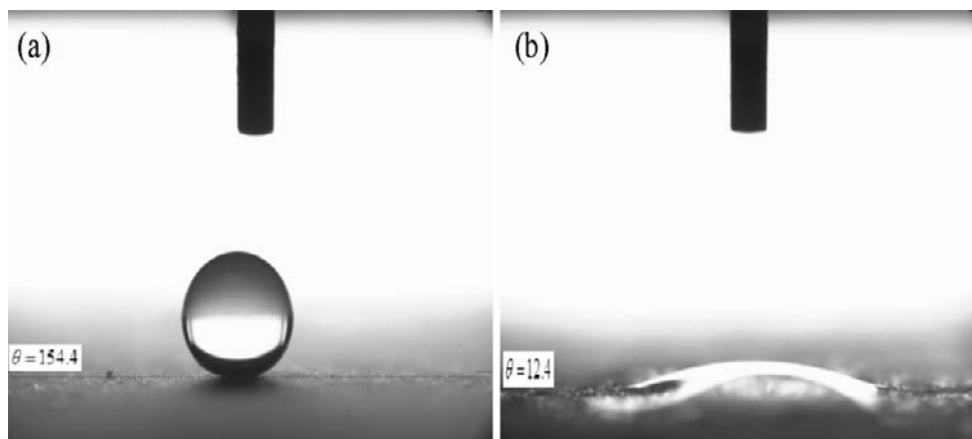
Figure 5. The water droplet on glass slides (a) coated with hydrophobic silica aerogels and (b) coated with hydrophilic silica aerogels.
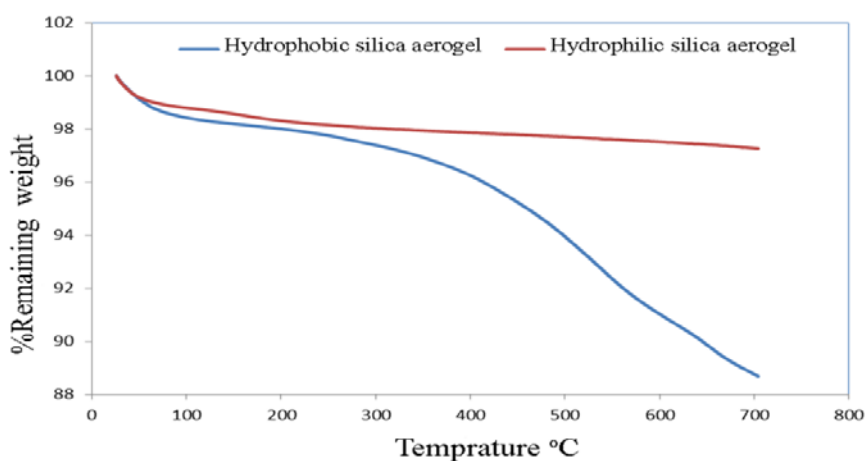
Figure 6. TGA test results of the hydrophobic and hydrophilic silica aerogels.
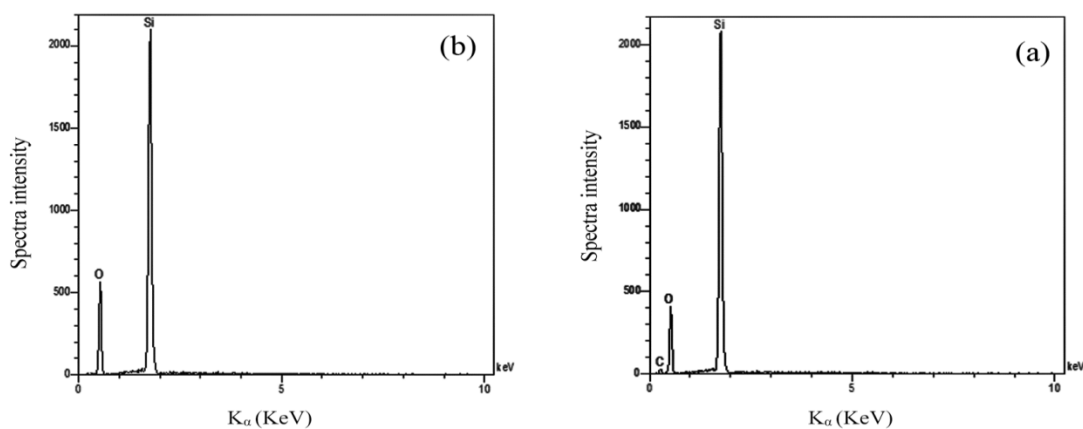

Figure 7. EDX spectrum plots for (a) hydrophobic silica aerogel and (b) hydrophilic silica aerogels.

## 3.1. Study of nitrate removal in the batch process

In the batch process using calcinated adsorbents, the pH level has a crucial role [35]. The effect of the pH level (range of 5-9) on the process is represented in Figure 8. The rise of the pH level in the solution (alkaline environment) causes an increment in the concentration of hydroxide which creates a competition to occupy the active sites [35]. Also, the pH level enhancement causes the electrostatic repulsion of the nitrate anion by the negatively charged surface of the adsorbent and this decreases the efficiency of the process [36, 37]. At low pH levels (acidic environment), there is a higher possibility of protonating the amine groups, resulting in a positively charged adsorbent [16]. Accordingly, the ion partition coefficient increases with pH that consequently increases the nitrate removal percentage [37].

The experimental results regarding the effects of the contact time on the nitrate removal percentage at pH=7, initial nitrate concentration=100 mg.L^{-1}, and adsorbent dosage=3 g are represented in Figure 9. As it is clear, after a contact time of 180 minutes, the removal percentage remains approximately constant and reaches its maximum.
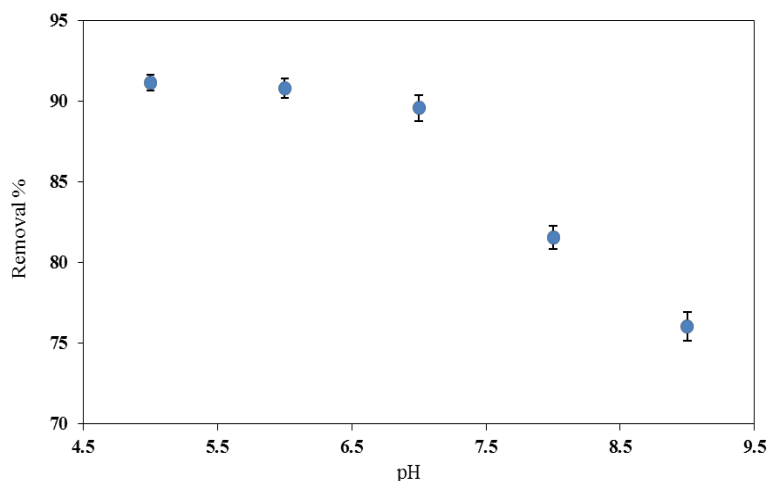
Figure 8. The effects of the pH level on the efficiency of the batch process. Initial nitrate concentration=100 mg.L^{-1}, contact time=180 min, and adsorbent dosage=3 g.
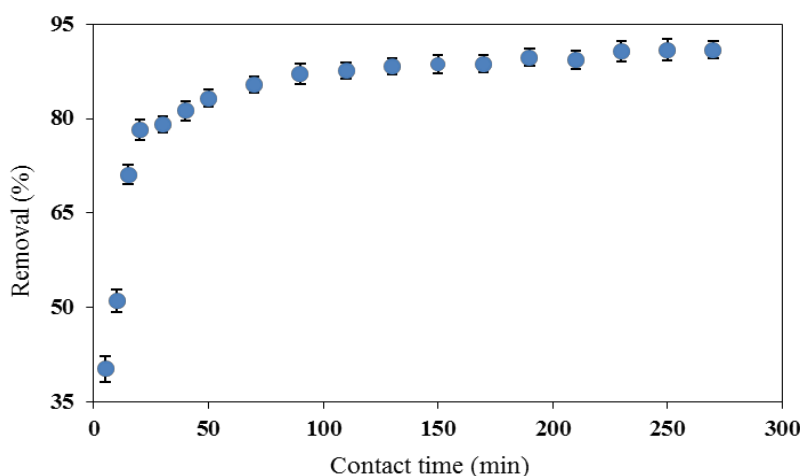
Figure 9. The effect of contact time on the efficiency of the batch process. Initial nitrate concentration=100 mg.L^{-1}, pH=7, and adsorbent dosage=3 g.
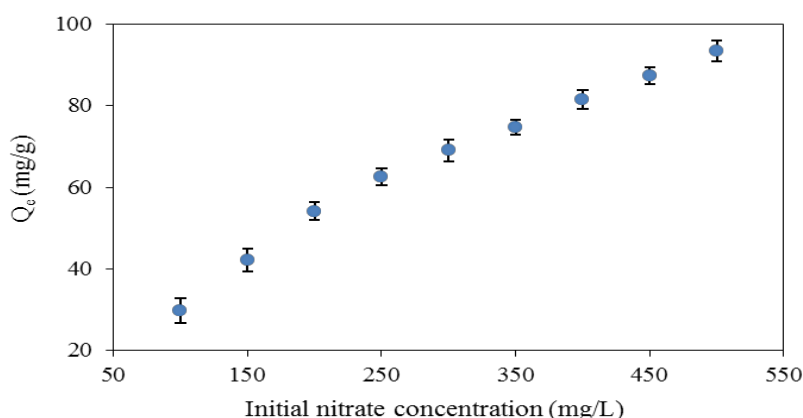
The effects of the initial nitrate concentration on the efficiency of the batch process were investigated using some nitrate solution samples (50-500 mg.L^{-1}, pH=7) comprising 3 g of the adsorbent. After 180 min, the solution was evaluated to indicate the final nitrate concentration. Finally, the equilibrium adsorption capacity (Q_e), which indicates the adsorbed nitrate (mg) per 1 gram of the adsorbent, was calculated through Equation (3) [38]:

$$Q_e = \frac{(C_0 - C_e) \times V}{m} \qquad (3)$$

where C_0 is the initial nitrate concentration (mg.L^{-1}), C_e denotes the equilibrium concentration of nitrate (mg.L^{-1}), V is the volume of the nitrate solution (L), and m is the adsorbent dosage (g). The results are represented in Figure 10. The increment of initial nitrate concentration increases the adsorbent capacity due to the availability of more nitrate anions which provides a higher driving force from anions to the active superficial sites of the adsorbents and also increases the collision probability [39].

For investigating the effects of adsorbent dosage on the process efficiency, different dosages of the adsorbent (1 to 7 g) were added to the prepared nitrate solution samples (initial nitrate concentration=100 mg.L^{-1}, and pH=7). Figure 11 depicts the test results of the contact time of 150 minutes. As it is clear, the increment of adsorbent dosage increases the removal percentage as a result of increase in the number of active sites [40].

Figure 10. The effect of the initial nitrate concentration on the equilibrium adsorption capacity. Adsorbent dosage=3 g, contact time=180 min, and pH=7.
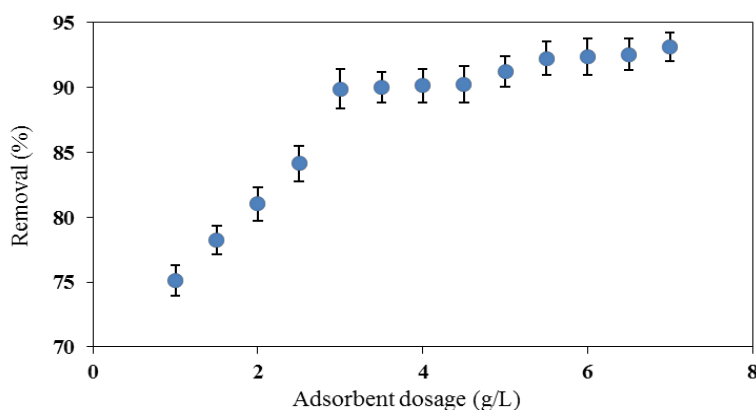
Figure 11. The effect of adsorbent dosage on the efficiency of the batch process. Initial nitrate concentration=100 mg.L^{-1}, contact time=180 min, and pH=7.

To define the theoretical nitrate removal percentage as a function of the initial nitrate concentration, the pH level, the adsorbent dosage, the process duration, and also their combinations, we used a second-order polynomial model as follows [41]:

$$R\% = \beta_0 + \sum_{i=1}^{4}\beta_0 x_i + \sum_{i=1}^{4}\sum_{j=1}^{4}\beta_{ij}x_i x_j + \sum_{i=1}^{4}\beta_{ii}x_i^2 \quad (4)$$

where β_0 is the model constant, β_i, β_{ij}, and β_{ii} are coefficients for the linear, quadratic, and cross products, respectively, x denotes different parameters such as initial nitrate concentration, contact time, adsorbent dosage, and pH level. The effective process parameters involved in Equation 4 were defined using variance analysis in which $p \leq 0.05$ defines the effectivity of a parameter [42, 43]. The results are represented in Table 1.

Table 1
The results of the variance analysis on model parameters. *C*, *AD*, and *t* stand for the initial nitrate concentration, the adsorbent dosage, and time, respectively.

	Parameters						
	C	pH	AD	t	C^2	pH^2	AD^2
P value	0.001	0.001	0.001	0.069	0.898	0.001	0.061
F value	112.22	78.72	52.11	3.93	0	16.011	4.01
	Parameters						
	t^2	C X pH	C X AD	C X t	pH X AD	pH X.t	AD X.t
P value	0.323	0.029	0.41	0.54	0.528	0.88	0.821
F value	0.88	4.59	0.22	0.39	0.612	0.07	0.13

It was revealed that the initial nitrate concentration (*C*), the adsorbent dosage (*AD*), the pH level, the initial nitrate concentration $\times$ pH, and pH $\times$ pH were the most effective parameters among the others (p<0.05), making it possible to rearrange the initial polynomial equation as follows:

$$R\% = 95.3 + 0.035 \times C + 11.78 \times pH - 8.19 \times AD$$
$$-1.312 \times pH^2 - 0.013 \times C \times pH \quad (5)$$

Applying a parameter optimization process to Equation (5) defines that the maximum nitrate removal percentage can be theoretically reached if the initial concentration is set to about 48 ppm, the time is set to 180 minutes, the adsorbent dosage is kept at 3 g, and the pH level is 6.7. Substituiting these values into Equation (5) resulted in the theoretical nitrate removal percentage of 94.7 % while applying them to an actual batch process removed 92.2 % of the nitrate, which was a good achievement. Moreover, the high F-values of both initial nitrate concentration and pH level make them even more effective among other effective ones (Table 1).

The equilibrium kinetic is used to study the adsorbent retention time and provide information about the required time to reach the maximum capacity of adsorption and the controlling mechanism in the process (e.g., mass transfer or chemical reactions) [16]. Accordingly, pseudo-first-order and pseudo-second-order kinetic models were used in order to investigate the kinetics of the batch nitrate removal process [44, 45]. The results of the pseudo first-order model (Equation (6)) are represented in Figure 12 and Table 2.

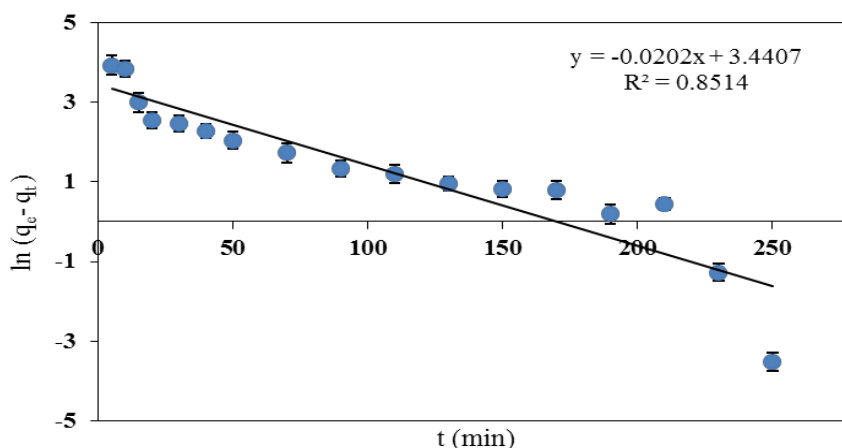$$\ln(q_e - q_t) = \ln(q_e) - k_1 t \quad (6)$$

where q_e (mg.g^{-1}) and q (mg.g^{-1}) denote the amounts of adsorbed nitrate at equilibrium

and at different time intervals, respectively. k_1 (min⁻¹) is the pseudo-first-order rate constant.

The results of the pseudo second-order model (Equation (7)) is represented in Figure 13 and Table 2.

$$\frac{t}{q_t} = \frac{1}{k_2 q_e^{\,2}} + \frac{t}{q_e} \qquad (7)$$

where k_2 (g.mg⁻¹.min⁻¹) denotes the pseudo-second-order rate constant.

Figure 12. Comparison of the results of the pseudo-first-order kinetic model and the experimental result at various initial nitrate concentrations.

Table 2
The rate constants of the applied kinetic models applied.

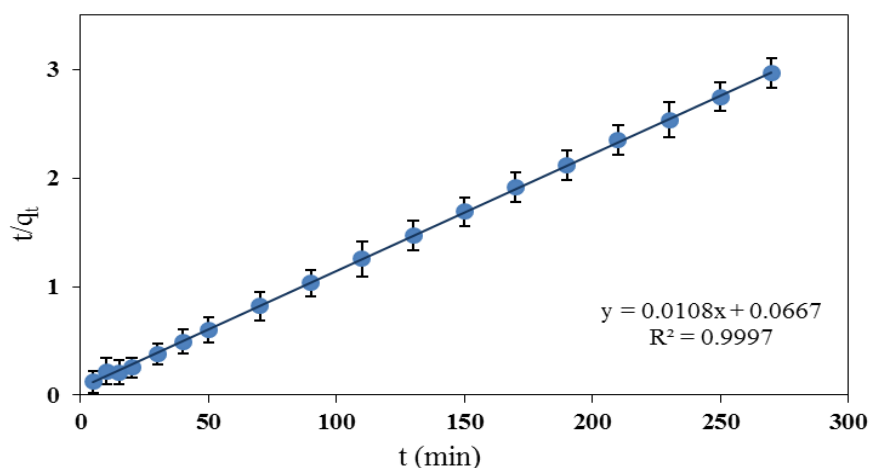| C_0 (mg l⁻¹)	Pseudo-first-order model			Pseudo-second-order model		
	k_1 (min⁻¹)	q_e (mg g⁻¹)	R^2	K_2 (g·min⁻¹mg⁻¹)	q_e (mg g⁻¹)	R^2
100	0.0202	31.20	0.8541	0.00174	92.59	0.9997

Figure 13. Comparison of the results of the pseudo-second-order kinetic model and the experimental result at various initial nitrate concentrations.

As it is shown in Figures 12 and 13, the pseudo-second-order rate model shows better agreement with the experimental results meaning that the chemical adsorption is the rate-limiting step of the process [46].

Adsorption isotherm defines the relation between the adsorbed quantity and the composition of the bulk phase, which is based

on the assumption that the adsorption sites are independent of each other [47, 48]. Accordingly, the results of Langmuir and Freundlich adsorption isotherm models were compared with experimental equilibrium data in order to define monolayer or multilayer nitrate adsorption on the surface of the adsorbents. The Langmuir model implies that each active site on the surface of the adsorbents is only capable of adsorbing one atom or molecule and also the surface of the adsorbent is completely uniform and homogenous [49]. The linear form of the applied Langmuir isotherm model is expressed by the following equation [9, 16, 36]:

$$\frac{C_e}{q_e} = \frac{1}{K_L q_m} + \frac{C_e}{q_m} \tag{8}$$

where q_e (mg.g^{-1}) is the equilibrium amount of the adsorbed nitrate, C_e (mg.L^{-1}) is the equilibrium nitrate concentration in the solution, q_m (mg.g^{-1}) denotes the maximum nitrate adsorption capacity, K_L (L.mg^{-1}) is the Langmuir adsorption equilibrium constant, and C_0 (mg.L^{-1}) is the initial nitrate concentration. The calculated values of q_m and K_L are presented in Table 3.

Table 3
The constants of the applied isotherm models.

| Langmuir isotherm			Freundlich isotherm		
q_m (mg g^{-1})	K_L (l mg^{-1})	R^2	K_F (l g^{-1})	n	R^2
104.17	0.026	0.987	13.30	2.75	0.968

The dimensionless constant separation factor (R_L) which determines whether the modeled adsorption process is favorable or not ($0<R_L<1$ represents a favorable adsorption process) can be expressed as follows [9, 36]:

$$R_L = \frac{1}{1 + K_L C_0} \tag{9}$$

where q_e (mg.g^{-1}) is the equilibrium amount of the adsorbed nitrate, C_e (mg.L^{-1}) is the equilibrium nitrate concentration in the solution, q_m (mg.g^{-1}) is the maximum nitrate adsorption capacity, K_L (L.mg^{-1}) is the Langmuir adsorption equilibrium constant, and C_0 (mg.L^{-1}) is the initial nitrate concentration.

As is clear from Figure 14, the experimental data are well fitted by Langmuir model, which suggests that the surface is homogeneous, the adsorption energy on the surface is uniform, and monolayer adsorption has occurred [9].
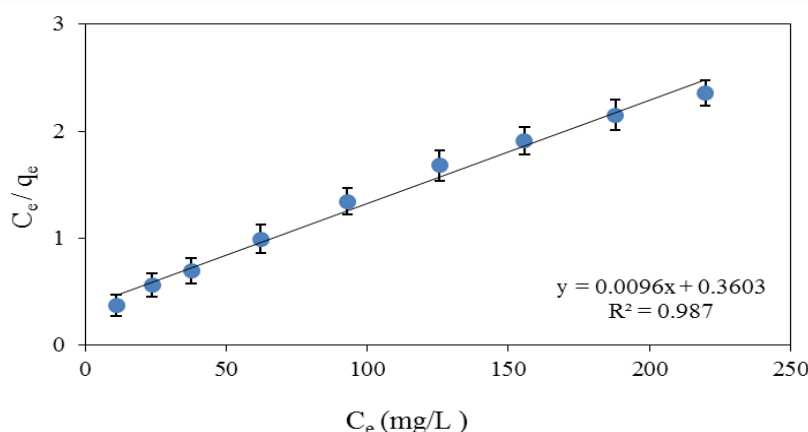
Figure 14. Comparison of the results of the Langmuir isotherm model and the experimental result.

Also, the diagram of R_L versus the initial nitrate concentration is represented in Figure 15. Accordingly, the R_L range (0.072 to 0.27) represents favorable nitrate adsorption based on the Langmuir isotherm model.

The linear form of the Freundlich isotherm model (Equation (10)) was used to investigate the multi-layer adsorption of nitrate on the surface of the adsorbents (Figure 16) [49].
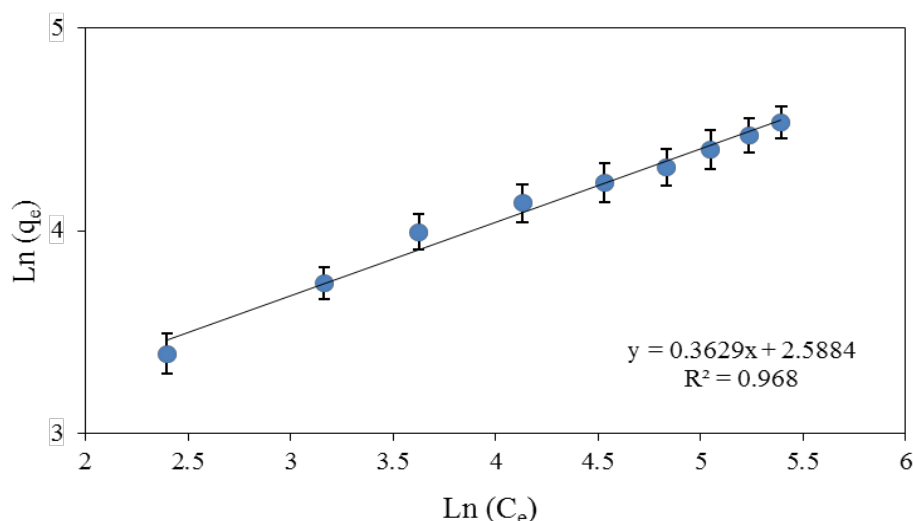
$$Ln\, q_e = Ln\, K_F + \frac{1}{n} Ln\, C_e \qquad (10)$$

where K_F (mg.g^{-1}) is the Freundlich adsorption isotherm constant (relating to adsorption capacity) and n denotes the adsorption intensity.
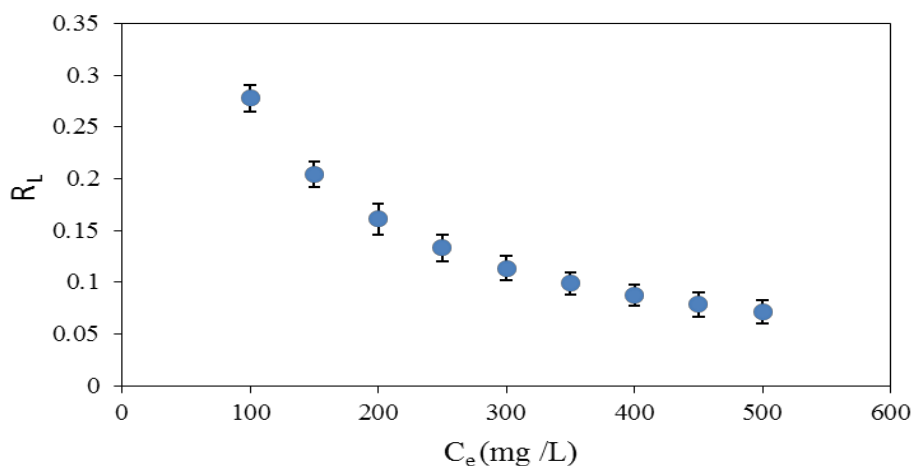
Figure 15. The variation of the dimensionless constant separation factor (R_L) versus C_e.

Figure 16. Comparison of the results of the Freundlich isotherm model and the experimental result.

In order to reach a favorable adsorption process, the value of n should be in the range of 1 to 10 [36, 50]. The calculated values of parameters K_F and n are listed in Table 3. As it is clear in Table 3, the regression coefficient (R^2) of the Freundlich model is less than that of the Langmuir model which confirms the monolayer adsorption of nitrate on the surface of the hydrophilic adsorbents.

3.2. Study of the nitrate removal in the continuous process

The effect of the bed height on the efficiency of the continuous process was investigated by

using two columns with 25 and 45 cm heights in which 4 and 7 g of the adsorbents were used, respectively (Figure 1). Similar initial nitrate concentration (100 mg.L^{-1}) and input flow rate (33.34 ml.min^{-1}) were applied in both setups. The variation of the ratio of the final output nitrate concentration to the initial nitrate concentration (C/C$_0$) versus time for both columns at ambient temperature is represented in Figure 17.
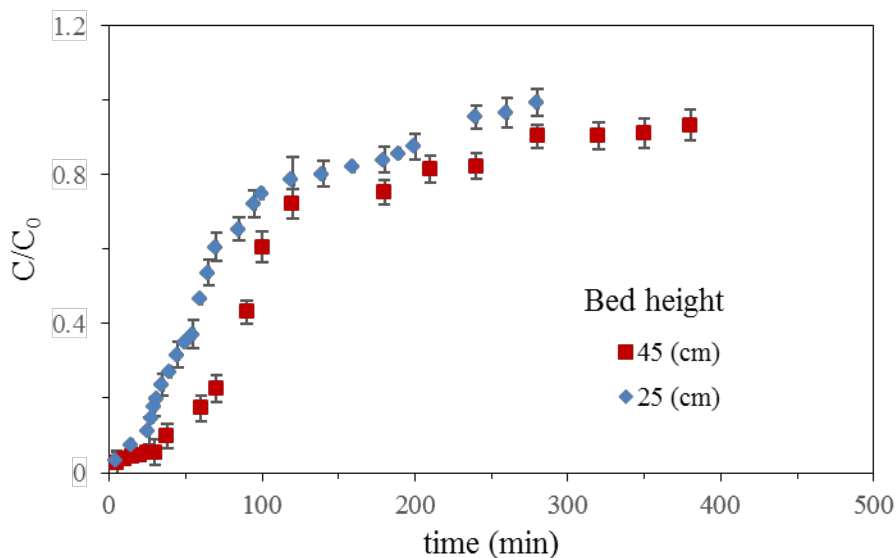
Figure 17. The effects of the variation of the bed height on the breakthrough curves.

The required time to reach the breakthrough point (t$_b$, when C/C$_0$ = 0.1) and saturation point (t$_s$, when C/C$_0$ = 1) increases with the bed height. The saturation time was measured to be 280 min and 380 min for 25 cm and 45 cm height columns, respectively. Moreover, the adsorbent capacities at the saturation point were 18.03 mg.g^{-1} and 18.22 mg.g^{-1} for 25 cm and 50 cm height columns, respectively. The variation trend of C/C$_0$ (as a function of time) at the interval of t$_b$ to t$_s$ is almost similar for both columns, meaning that the variation in the bed height only shifts t$_b$ and t$_s$. This phenomenon is attributed to the constant nitrate concentration in the input flow, which results in a similar concentration gradient and the similar required length of the mass transfer zone in both columns [51]. Accordingly, it can be concluded that in the case of applying constant nitrate concentration in the feed, the bed height has no significant effect on the final efficiency of

the continuous nitrate removal process [51].

The effect of the input flow rate on the efficiency of the continuous process was investigated using a 25 cm height column with different input flow rates of 16.67 and 33.34 mL.min^{-1} comprising constant initial nitrate concentration of 100mg.L^{-1}. As it is demonstrated in Figure 18, the increment of the input flow rate increases the stream velocity through the adsorption column and consequently reduces the empty bed contact time (EBCT) (Figure 18). This slows down the diffusion process as the controlling parameter of the nitrate adsorption (more time is required for creating bonds between the adsorbents and nitrate anions) [52]. On the other hand, increasing the flow rate causes the adsorbents to be saturated more quickly, which consequently shortens the contact time between the nitrate ions and the adsorbent and imposes more nitrate load on the column in the unit of time [53]. Moreover, it was

revealed that as the zone speed increased with the flow rate, the system reached breakthrough point faster. The measured adsorbent capacities (q_{sat}) were 20.46 and 18.03 mg.g^{-1} in columns with input flow rates of 16.67 and 33.34 ml.min^{-1}, respectively.
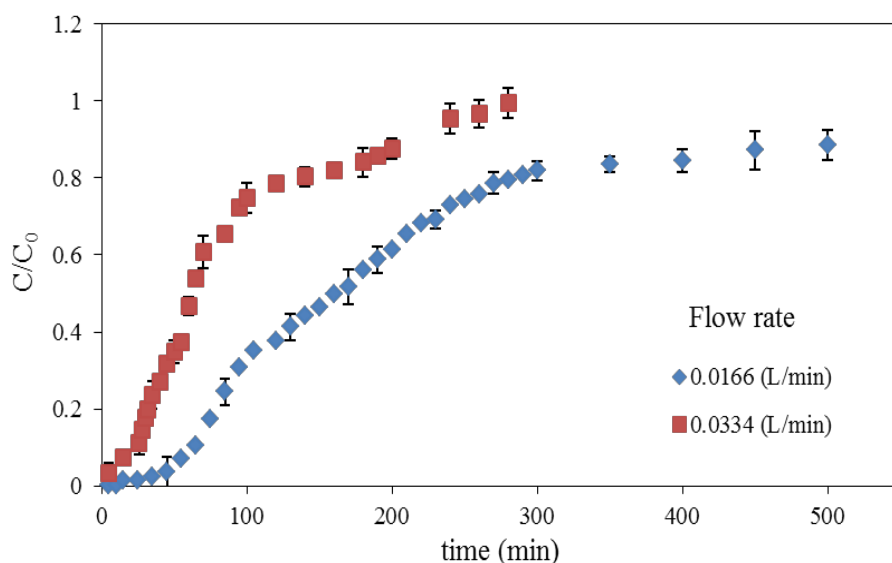
Figure 18. The effects of the variation in the flow rate on the breakthrough curves.

The effect of the variation in initial nitrate concentration on the breakthrough curves is represented in Figure 19. The related experiments were performed in the height column of 25 cm with a constant flow rate of 16.67 ml.min^{-1} comprising different initial nitrate concentrations of 100 and 200 mg.L^{-1}.
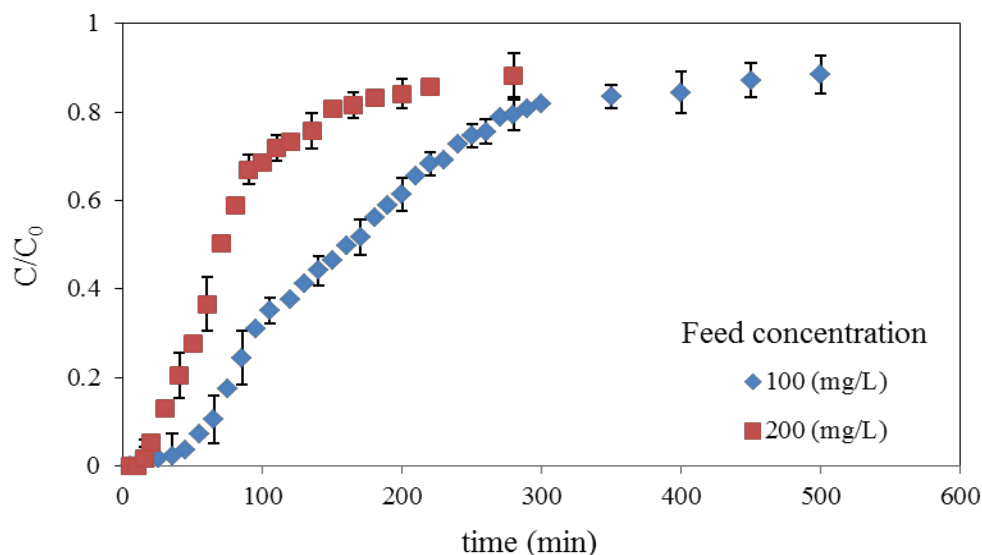
Figure 19. The effects of the variation in the initial nitrate concentration on breakthrough curve.

As it is clear, the slope of the breakthrough curves and the breakthrough times (t_b) decrease with the increment of the initial nitrate concentration (t_b was measured to be 65 and 30 min corresponding to the initial nitrate concentrations of 100 and 200 mg.L^{-1}, respectively). This can be attributed to the increased loading rate of nitrate anions onto

the adsorbent surface. It can be said that the diffusion phenomenon depends on the concentration of the feed. Nitrate loading rate increases by increasing the concentration of the feed. On the other hand as the loading rate increases, the driving force of mass transfer decreases over the length of the absorption zone. The net effect of these two phenomena leads to an increase in adsorption capacity. Additionally, it can be declared that the amount of available nitrate ions in the column increases by increasing nitrate concentration [54]. The adsorbent capacities (q_{sat}) were measured to be 20.46 and 21.05 mg.g^{-1} corresponding to the initial nitrate concentrations of 100 and 200 mg.L^{-1}, respectively. These results showed that the variation of initial nitrate concentration in the input feed had a trivial effect on q_{sat} [51].

4. Conclusions

Silica aerogel was synthesized by sol-gel method and ambient pressure drying. Then, the effects of different parameters on the efficiency of the adsorption processes of the nitrate anion (batch and continuous) onto the surface of the calcined silica aerogels were evaluated. The results showed that the maximum absorption in the batch process occurred by 3 grams of adsorbent (for a concentration of 100 mg.L^{-1}) and lasted for 180 minutes and the decrease of the pH level up to pH ≈ 6 increased the removal percentage while after that (i.e acidic environment), removal percentage decreased. This phenomenon was attributed to the formation of the positively charged surface of the adsorbents, which mostly occurred at low pH levels [16]. Increasing the contact time and the adsorbent dosage increased the removal efficiency while increasing the initial nitrate concentration decreased it. Also, Langmuir

and Freundlich isotherm models were used in order to investigate the adsorption isotherms and according to the obtained results, the Langmuir model was in better agreement with the experimental data. Nitrate adsorption kinetics was explained well via the pseudo-second-order kinetics model which indicated that the chemical adsorption was the controlling mechanism of the adsorption process.

Finally, in the continuous process, the adsorbent capacities (q_{sat}) were measured to be 20.46 and 21.05 mg.g^{-1} for increasing initial nitrate concentration (from 100 to 200 mg.L^{-1}) and the measured adsorbent capacities (q_{sat}) were 20.46 and 18.03 mg.g^{-1} for the input flow rate experiments in the columns. Furthermore, it was proved that increasing the bed height did not drastically affect the adsorbent capacity while it increased the time to reach breakthrough and exhaustion points.

Nomenclature

C_0	initial nitrate concent.
C_t	variable concentration with time.
C_e	the equilibrium nitrate concentration in the solution [mg.L^{-1}].
K_L	the Langmuir adsorption equilibrium constant [L.mg^{-1}].
K_F	the Freundlich adsorption isotherm constant [mg.g^{-1}].
k_1	the pseudo-first order rate constant [min^{-1}].
k_2	the pseudo-second-order rate constant [mg.g^{-1}.min^{-1}].
m	adsorbent mass.
n	the adsorption intensity.
Q	the input flow rate.
q_e	the equilibrium amount of nitrate adsorbed

by Hydrophilic silica aerogel [mg.g^{-1}].

q_m denotes the maximum nitrate adsorption capacity [mg.g^{-1}].

q_t the amounts of adsorbed nitrate [mg.g^{-1}].

R %   removal percentage.

R_L the dimensionless constant separation factor.

t_{sat} saturation time.

t_b breakthrough time.

β_0 second-order polynomial model constant.

β_i coefficients for the linear product.

β_{ij} coefficients for the quadratic product.

β_{ii} coefficients for the cross product.

χ^2 chi-square error function.

References

[1] Moore, J. W., Inorganic contaminants of surface water: Research and monitoring priorities, Springer Science & Business Media, (2012).

[2] Bhatnagar, A., Kumar, E. and Sillanpää, M., "Nitrate removal from water by nano-alumina: Characterization and sorption studies", *Chemical Engineering Journal*, **163** (3), 317 (2010).

[3] Organization, W. H., Guidelines for drinking-water quality: Recommendations, World Health Organization, (2004).

[4] Majumdar, D. and Gupta, N., "Nitrate pollution of groundwater and associated human health disorders", *Indian Journal of Environmental Health*, **42** (1), 28 (2000).

[5] Mena-Duran, C., Kou, M. S., Lopez, T., Azamar-Barrios, J., Aguilar, D., Dominguez, M., Odriozola, J. and Quintana, P., "Nitrate removal using natural clays modified by acid thermoactivation", *Appl. Surf. Sci.*, **253** (13), 5762 (2007).

[6] Kapoor, A. and Viraraghavan, T., "Nitrate removal from drinking water", *Journal of Environmental Engineering*, **123** (4), 371 (1997).

[7] Selecky, M., Adair, J. and Clifford, D., "Nitrate treatment alternatives for small water systems", Department of Health, Washington, (2005).

[8] Singh, N., Nagpal, G. and Agrawal, S., "Water purification by using adsorbents: A review", *Environmental Technology & Innovation*, **11**, 187 (2018).

[9] Zhan, Y., Lin, J. and Zhu, Z., "Removal of nitrate from aqueous solution using cetylpyridinium bromide (CPB) modified zeolite as adsorbent", *Journal of Hazardous Materials*, **186** (2), 1972 (2011).

[10] Afkhami, A., Madrakian, T. and Karimi, Z., "The effect of acid treatment of carbon cloth on the adsorption of nitrite and nitrate ions", *Journal of Hazardous Materials*, **144** (1), 427 (2007).

[11] Mena-Duran, C., Kou, M. S., Lopez, T., Azamar-Barrios, J., Aguilar, D., Dominguez, M., Odriozola, J. A. and Quintana, P., "Nitrate removal using natural clays modified by acid thermoactivation", *Applied Surface Science*, **253** (13), 5762 (2007).

[12] Bergaya, F., Theng, B. K. G. and Lagaly, G., Handbook of clay science, Elsevier Science, Netherlands, (2011).

[13] Inglezakis, V. J. and Zorpas, A. A., Handbook of natural zeolites, Bentham Science Publishers, (2012).

[14] Liu, J., Cheng, X., Zhang, Y., Wang, X., Zou, Q. and Fu, L., "Zeolite modification for adsorptive removal of nitrite from aqueous solutions", *Microporous Mesoporous Mater.*, **252**, 179 (2017).

[15] Zhu, I. and Getting, T., "A review of nitrate reduction using inorganic materials", *Environmental Technology*

Reviews, **1** (1), 46 (2012).

[16] Chatterjee, S. and Woo, S. H., "The removal of nitrate from aqueous solutions by chitosan hydrogel beads", *J. Hazard. Mater.*, **164** (2), 1012 (2009).

[17] Masheane, M. L., Nthunya, L. N., Sambaza, S. S., Malinga, S. P., Nxumalo, E. N., Mamba, B. B. and Mhlanga, S. D., "Chitosan-based nanocomposite beads for drinking water production", *IOP Conference Series: Materials Science and Engineering*, **195** (1), 012004 (2017).

[18] Nazeran, N. and Moghaddas, J. S., "Synthesis and characterization of silica aerogel reinforced rigid polyurethane foam for thermal insulation application", *Journal of Non-Crystalline Solids*, **461**, 1 (2017).

[19] Rezaei, E. and Moghaddas, J. S., "Thermal conductivities of silica aerogel composite insulating material", *Advanced Materials Letters*, **7** (4), 296-301, (2016).

[20] Liu, H., Sha, W., Cooper, A. T. and Fan, M., "Preparation and characterization of a novel silica aerogel as adsorbent for toxic organic compounds", *Colloids and Surfaces A: Physicochemical and Engineering Aspects*, **347** (1), 38 (2009).

[21] Armstrong, F., "Determination of nitrate in water ultraviolet spectrophotometry", *Analytical Chemistry*, **35** (9), 1292 (1963).

[22] Khani, A. and Mirzaei, M., "Comparative study of nitrate removal from aqueous solution using powder activated carbon and carbon nanotubes", *Poceedigs of 2nd International IUPAC Conference on Green Chemistry,* Russia, (2008).

[23] Islam, M., "Development of adsorption media for removal of lead and nitrate from water", Ph. D. Thesis, National Institute of Technology, Rourkela, (2008).

[24] Schick, J., Caullet, P., Paillaud, J. -L., Patarin, J. and Mangold-Callarec, C., "Nitrate sorption from water on a surfactant-modified zeolite. fixed-bed column experiments", *Microporous Mesoporous Mater.*, **142** (2), 549 (2011).

[25] McCabe, W. L., Smith, J. C. and Harriott, P., Unit operations of chemical engineering, Vol. 5, McGraw-Hill, New York, (1993).

[26] Thomas, W. J. and Crittenden, B. D., Adsorption technology and design, Butterworth-Heinemann, (1998).

[27] Mantovaneli, I., Ferretti, E., Simões, M. and Silva, C., "The effect of temperature and flow rate on the clarification of the aqueous stevia-extract in a fixed-bed column with zeolites", *Braz. J. Chem. Eng.*, **21** (3), 449 (2004).

[28] Sarawade, P. B., Kim, J. -K., Hilonga, A., Quang, D. V., Jeon, S. J. and Kim, H. T., "Synthesis of sodium silicate-based hydrophilic silica aerogel beads with superior properties: Effect of heat-treatment", *J. Non-Cryst. Solids*, **357** (10), 2156 (2011).

[29] Falahnejad, M., Mousavi, H. Z., Shirkhanloo, H. and Rashidi, A., "Preconcentration and separation of ultra-trace amounts of lead using ultrasound-assisted cloud point-micro solid phase extraction based on amine functionalized silica aerogel nanoadsorbent", *Microchem. J.*, **125**, 236 (2016).

[30] Sharifzadeh, E., Salami-Kalajahi, M., Hosseini, M. S. and Aghjeh, M. K. R., "A temperature-controlled method to

produce Janus nanoparticles using high internal interface systems: Experimental and theoretical approaches", *Colloids and Surfaces A: Physicochemical and Engineering Aspects*, **506**, 56 (2016).

[31] Sharifzadeh, E., Salami-Kalajahi, M., Hosseini, M. S. and Aghjeh, M. K. R., "Synthesis of silica Janus nanoparticles by buoyancy effect-induced desymmetrization process and their placement at the PS/PMMA interface", *Colloid. Polym. Sci.*, **295** (1), 25 (2017).

[32] Rao, A. P., Rao, A. V. and Pajonk, G., "Hydrophobic and physical properties of the ambient pressure dried silica aerogels with sodium silicate precursor using various surface modification agents", *Appl. Surf. Sci.*, **253** (14), 6032 (2007).

[33] Sharifzadeh, E., Salami-Kalajahi, M., Hosseini, M. S., Aghjeh, M. K. R., Najafi, S., Jannati, R. and Hatef, Z., "Defining the characteristics of spherical Janus particles by investigating the behavior of their corresponding particles at the oil/water interface in a Pickering emulsion", *J. Dispersion Sci. Technol.*, **38** (7), 985 (2017).

[34] Jeong, A. -Y., Koo, S. -M. and Kim, D. -P., "Characterization of hydrophobic SiO$_2$ powders prepared by surface modification on wet gel", *J. Sol-Gel Sci. Technol.*, **19** (1), 483 (2000).

[35] Su, J. F., Shi, J. X., Huang, T. L., Ma, F., Lu, J. S. and Yang, S. F., "Effect of nitrate concentration, pH, and hydraulic retention time on autotrophic denitrification efficiency with Fe(II) and Mn(II) as electron donors", *Water Science and Technology : A Journal of the International Association on Water Pollution Research*, **74** (5), 1185 (2016).

[36] Chatterjee, S., Lee, D. S., Lee, M. W. and Woo, S. H., "Nitrate removal from aqueous solutions by cross-linked chitosan beads conditioned with sodium bisulfate", *J. Hazard. Mater.*, **166** (1), 508 (2009).

[37] Jaafari, K., Ruiz, T., Elmaleh, S., Coma, J. and Benkhouja, K., "Simulation of a fixed bed adsorber packed with protonated cross-linked chitosan gel beads to remove nitrate from contaminated water", *Chem. Eng. J.*, **99** (2), 153 (2004).

[38] Vasconcelos, H. L., Camargo, T. P., Gonçalves, N. S., Neves, A., Laranjeira, M. C. and Fávere, V. T., "Chitosan crosslinked with a metal complexing agent: Synthesis, characterization and copper (II) ions adsorption", *React. Funct. Polym.*, **68** (2), 572 (2008).

[39] Baldrian, P., "Interactions of heavy metals with white-rot fungi", *Enzyme Microb. Technol.*, **32** (1), 78 (2003).

[40] Onyango, M. S., Masukume, M., Ochieng, A. and Otieno, F., "Functionalised natural zeolite and its potential for treating drinking water containing excess amount of nitrate", *Water SA*, **36** (5), 655 (2010).

[41] Roosta, M., Ghaedi, M., Shokri, N., Daneshfar, A., Sahraei, R. and Asghari, A., "Optimization of the combined ultrasonic assisted/adsorption method for the removal of malachite green by gold nanoparticles loaded on activated carbon: Experimental design", *Spectrochimica Acta Part A: Molecular and Biomolecular Spectroscopy*, **118**, 55 (2014).

[42] Ghanbarian, S., Kahforoushan, D. and Sahraei, E., "Determination of significant factors in the removal of Cu (II) from aqueous solutions by applying adsorption

method: Using factorial design", *Desalin. Water Treat.*, **57** (18), 8470 (2016).

[43] Montgomery, D. C., Design and analysis of experiments, John Wiley & Sons, (2008).

[44] Yuh-Shan, H., "Citation review of Lagergren kinetic rate equation on adsorption reactions", *Scientometrics*, **59** (1), 171 (2004).

[45] Ho, Y. S., "Review of second-order models for adsorption systems", *Journal of Hazardous Materials*, **136** (3), 681 (2006).

[46] Ho, Y. -S. and McKay, G., "Pseudo-second order model for sorption processes", *Process Biochem.*, **34** (5), 451 (1999).

[47] Katal, R., Baei, M. S., Rahmati, H. T. and Esfandian, H., "Kinetic, isotherm and thermodynamic study of nitrate adsorption from aqueous solution using modified rice husk", *Journal of Industrial and Engineering Chemistry*, **18** (1), 295 (2012).

[48] Bleam, W. F., Soil and environmental chemistry, Elsevier Science, (2011).

[49] Ruthven, D. M., Principles of adsorption and adsorption processes, John Wiley & Sons, (1984).

[50] Senturk, H. B., Ozdes, D., Gundogdu, A., Duran, C. and Soylak, M., "Removal of phenol from aqueous solutions by adsorption onto organomodified Tirebolu bentonite: Equilibrium, kinetic and thermodynamic study", *J. Hazard. Mater.*, **172** (1), 353 (2009).

[51] Xing, X., Gao, B. -Y., Zhong, Q. -Q., Yue, Q. -Y. and Li, Q., "Sorption of nitrate onto amine-crosslinked wheat straw: Characteristics, column sorption and desorption properties", *J. Hazard. Mater.*, **186** (1), 206 (2011).

[52] Sarin, V., Singh, T. S. and Pant, K., "Thermodynamic and breakthrough column studies for the selective sorption of chromium from industrial effluent on activated eucalyptus bark", *Bioresource Technology*, **97** (16), 1986 (2006).

[53] Salman Tabrizi, N. and Yavari, M., "Fixed bed study of nitrate removal from water by protonated cross-linked chitosan supported by biomass-derived carbon particles", *Journal of Environmental Science and Health, Part A*, 1 (2020).

[54] Kang, J. -K., Lee, S. -C. and Kim, S. -B., "Synthesis of quaternary ammonium-functionalized silica gel through grafting of dimethyl dodecyl [3-(trimethoxysilyl) propyl] ammonium chloride for nitrate removal in batch and column studies", *Journal of the Taiwan Institute of Chemical Engineers*, **102**, 153 (2019).